SCIENTIFIC REPORTS

OPEN

SUBJECT AREAS:
SCANNING PROBE MICROSCOPY
TWO-DIMENSIONAL MATERIALS

Received
23 April 2014

Accepted
8 July 2014

Published
4 August 2014

Correspondence and requests for materials should be addressed to J.-L.Z. (zuojl@nju.edu.cn); Q.-D.Z. (zengqd@nanoctr.cn) or K.D. (kdeng@nanoctr.cn)

Tetrathiafulvalene-Supported Triple-Decker Phthalocyaninato Dysprosium(III) Complex: Synthesis, Properties and Surface Assembly

Feng Gao[1], Xue-Mei Zhang[2], Long Cui[1], Ke Deng[2], Qing-Dao Zeng[2] & Jing-Lin Zuo[1]

[1]State Key Laboratory of Coordination Chemistry, School of Chemistry and Chemical Engineering, Nanjing National Laboratory of Microstructures, Nanjing University, Nanjing, 210093, P.R. China, [2]CAS Key Laboratory of Standardization and Measurement for Nanotechnology, National Center for Nanoscience and Technology, Beijing, 100190, P.R. China.

Self-assembly of functional compounds into a prerequisite nanostructure with desirable dimension and morphology by controlling and optimizing intermolecular interaction attracts an extensive research interest for chemists and material scientist. In this work, a new triple-decker sandwich-type lanthanide complex with phthalocyanine and redox-active Schiff base ligand including tetrathiafulvalene (TTF) units has been synthesized, and characterized by single crystal X-ray diffraction analysis, absorption spectra, electrochemical and magnetic measurements. Interestingly, the non-centrosymmetric target complex displays a bias dependent selective adsorption on a solid surface, as observed by scanning tunneling microscopy (STM) at the single molecule level. Density function theory (DFT) calculations are utilized to reveal the formation mechanism of the molecular assemblies, and show that such electrical field dependent selective adsorption is regulated by the interaction between the external electric field and intrinsic molecular properties. Our results suggest that this type of multi-decker complex involving TTF units shows intriguing multifunctional properties from the viewpoint of structure, electric and magnetic behaviors, and fabrication through self-assembly.

With the development of science and technology, the investigation and application of new functional materials have been the main task for production and life. Single-molecule magnets (SMMs) as molecular species exhibiting quantum tunneling and slow magnetic-relaxation processes, have been investigated from the viewpoint of applied science for use in next-generation devices, such as memory storage, quantum computers and spin-based molecular electronics[1–5]. As a representative, sandwich-type phthalocyaninato and/or porphyrinato lanthanide complexes possess intriguing molecular structures, unique electronic and optical properties due to intramolecular interactions and intrinsic nature of the metal ion[6–11], rendering them potentially useful in material science, including molecular spintronics, chemical sensors and field-effect transistors[12–16]. Self-assembly of these functional molecules into a prerequisite nanostructure with desirable dimension and morphology via controlling and optimizing intermolecular interaction has been a subject of extensive research interest for chemists and material scientist[17–20].

Recently, the need for new materials with more diversified and more sophisticated properties is continuously increasing. One of the goals is to prepare materials that possess not only one expected property or function but also combine two or more of them in one system. In particular, owing to the important applications in molecular spintronics, the synthesis of novel materials possessing synergy or interplay between electrical conductivity with magnetism has attracted attention in the last few years[21–25]. Tetrathiafulvalene (TTF) and its derivatives, well-known sulfur-rich organic molecules, are ideally suited as components in these types of systems because they can act as reversible and stable electron donors. Their cationic radical salts constitute an important class of conducting molecular materials[26–29], and have been incorporated as units on molecular machines[30–31]. Absorbing redox-active TTF organic units on surfaces, and assembling SMMs systems comprised of these molecules with the paramagnetic metal ions may lead to new multifunctional materials with interesting structures and properties[26,32–40].

Herein, we report the synthesis and surface assembly of the first sandwich-type triple-decker lanthanide complex based on a Schiff base ligand containing electrochemically active TTF unit H_2L (H_2L = 2,2′-((2-(4,5-

bis(methylthio)-1,3-dithiol-2-ylidene)-1,3-benzodithiole-5,6-diyl)-bis(nitrilomethylidyne)bis(4-chlorophenol)), which extends the classical system of sandwich-type tetrapyrrole oligomers limited to homoleptic or heterolepic phthalocyanine and/or porphyrin lanthanide multi-decker complexes[6–11]. For future applications in molecular electronics or spintronics, such as molecular field-effect transistors or spin field-effect transistors, the introduction of redox-active TTF derivatives will offer opportunities for new multifunctional molecular materials to fabricate single-molecule devices.

Results

Reaction of phthalocyanine, dysprosium acetylacetonate and TTF-supported Schiff base ligand in a 1 : 2 : 2 molar ratio in 1,2-dichloroethane and methanol resulted into the formation of target complex $[Dy_2(Pc)L_2(CH_3OH)]\cdot 5(ClCH_2CH_2Cl)$ (complex **1**, Supplementary Fig. S1), which is stable in both solution and solid state, and corresponding characterization has been accomplished by single crystal X-ray diffraction analysis, absorption spectra, electrochemical and magnetic measurements. More interestingly, the assembling behavior of such novel complex was studied by scanning tunneling microscopy (STM) on a highly oriented pyrolytic graphite (HOPG) surface, for probing the surface patterns and revealing the interface information at the single-molecule level.

Molecule structural description. Complex **1** crystallizes in the triclinic space group *P*$\bar{1}$ with the unique non-centrosymmetric tripler-decker sandwich-type molecular structure. As shown in Fig. 1, the Dy1 ion is eight-coordinated to six N atoms (four from the Pc and two from the H_2L) and two phenolic O atoms, while the seven-coordinated Dy2 ion is surrounded by two N atoms of another TTF-supported Schiff base ligand and five O atoms (four from the H_2L and one from a methanol molecule). Employing Continuous Shape Measures (CShMs) method[41] allows us to determine the degree of distortion of the Dy(III) coordination sphere (Supplementary Table S1). The results show that the coordination geometry of Dy1 ion can be described as a similar square antiprism (SAPR) with *S* value of 0.928 (The *S* values indicate the proximity to the ideal polyhedron, $S = 0$ corresponds to the non-distorted polyhedron), while seven-coordinated Dy2 adopts a conformation close to a capped trigonal prism (CTPR). The two Dy^{3+} ions are bridged by the O1 and O2 atoms with Dy1···Dy2 distance of 3.887(5) Å. The dihedral angles between the mean planes of N1-N3-N5-N7 and O1-O2-N9-N10, O1-O2-N9-N10 and O3-O4-N11-N12, N1-N3-N5-N7 and O3-O4-N11-N12, are 1.10(15)°, 17.09(17)°, and 16.02(19)°, respectively. Two TTF cores adopt boat-like conformation, and the average deviation from a least-squares plane for one TTF core containing S1, S2, S3 and S4 atoms is 0.365 Å, while another TTF core containing S7, S8, S9 and S10 atoms is a deviation of 0.157 Å, indicating the distortion of TTF-supported Schiff base ligand in the middle layer is larger than that in the bottom layer. In the crystal packing (Supplementary Fig. S2), a wave-shaped conformation can be observed due to the different distortion of the TTF units, and the shortest intermolecular distance between the two Dy^{3+} ions is 8.541(6) Å without showing significant intermolecular interactions and shorter S···S contacts.

Electrochemical and spectroscopic properties. Electrochemical properties were investigated by cyclic voltammetry (Supplementary Fig. S3). The H_2L ligand and complex **1** show similar two-step reversible oxidation processes, suggesting the presence of redox activities in present system. Additionally, UV-Vis absorption spectrum for complex **1** shows typical feature of phthalocyaninate metal complexes with a strong Q band around 686 nm and an additional weak absorption at about 615 nm (Supplementary Fig. S4), originating from the π-π* transitions of the phthalocyaninate ligand[42].

Static and dynamic magnetic properties. The static magnetic behaviors for complex **1** were investigated under 100 Oe direct current (dc) magnetic field. As shown in Fig. 2a, the $\chi_M T$ value of 27.55 cm^3 K mol^{-1} at 300 K is slightly smaller than the theoretical value for two uncoupled Dy(III) ions (28.34 cm^3 K mol^{-1}, $^6H_{15/2}$, $S = {}^5/_2$, $L = 5$, $J = {}^{15}/_2$, $g = {}^4/_3$). When the temperature is lowered, the $\chi_M T$ value drops to a minimum value of 23.52 cm^3 K mol^{-1} at about 6.0 K, mainly ascribed to the progressive depopulation of excited Stark sublevels of Dy(III)[10,43]. Upon further cooling, the curve increases abruptly again and reaches a maximum value of 24.58 cm^3 K mol^{-1} at 1.8 K, likely due to the weak ferromagnetic Dy(III)-Dy(III) interactions[44]. Field-dependent magnetization for complex **1** increases rapidly at low fields (Fig. 2a, Inset), and then achieves a maximum value of 11.96 Nβ at 70 kOe without reaching the theoretical saturation value (20 Nβ for two isolated Dy(III) ions), indicating the presence of the crystal-field effects and magnetic anisotropy for Dy(III) ion in this sandwich system[45].

Alternating current (ac) susceptibility measurements were carried out to study the dynamics of the magnetization for **1** (Supplementary Figs. S5 and S6). The temperature dependence of ac magnetic susceptibilities exhibit obvious frequency-dependent character in the in-phase (χ') and out-of-phase (χ'') signals under $H_{dc} = 0$ Oe and $H_{ac} = 2$ Oe. Nevertheless, no maxima of χ'' signals were observed

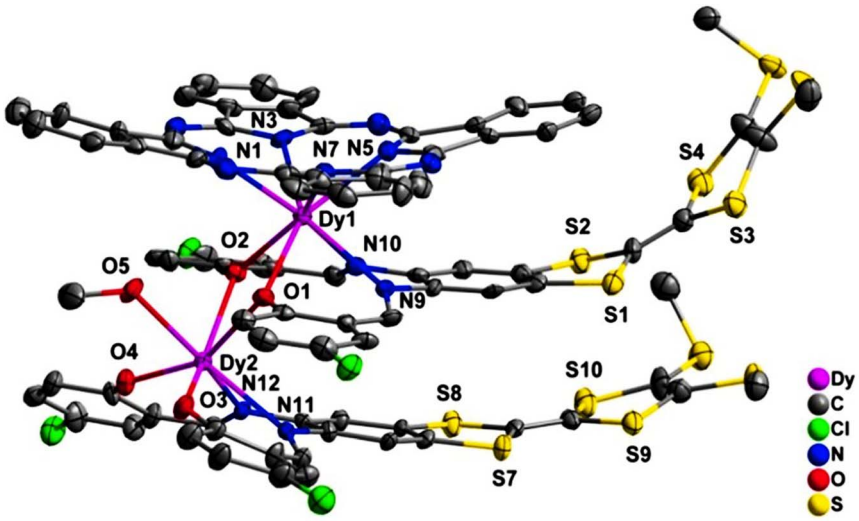

Figure 1 | Molecular structure for complex 1 with thermal ellipsoids at 30% probability. Hydrogen atoms and solvent molecules are omitted for clarity.

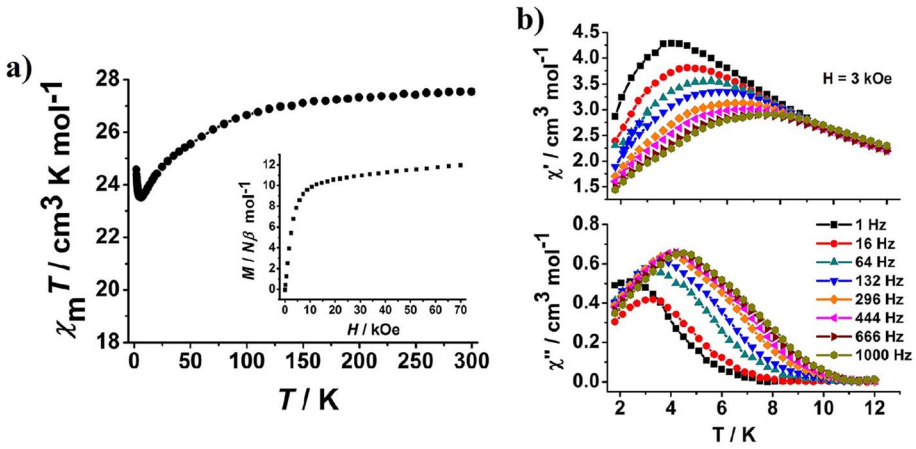

Figure 2 | (a) Temperature-dependent $\chi_M T$ values for complex **1** under 100 Oe dc field. Inset: Field-dependent magnetization plots for 1 at 1.8 K. (b) Temperature dependence of the in-phase and out-of-phase ac magnetic susceptibilities for **1** under 3 kOe dc field in the frequency range 1–1000 Hz.

above 1.8 K owing to the fast relaxation associated with the quantum tunneling at zero magnetic field. Such behavior is attributed to the degeneracy of the ground Kramers states of each single Dy(III) ion, which is consistent with some similar Dy-SMMs[10,44]. Performing an applied dc field of 3 kOe, the peaks of χ'' signals in the temperature-dependent ac susceptibilities clearly appear at frequencies as low as 16 Hz (Fig. 2b), indicating field induced SMM behavior with the suppression of the quantum tunneling of the magnetization (QTM) between sublevels. Furthermore, there are probably associated with the interesting dynamic magnetic behavior due to the slightly distinct anisotropic Dy(III) centers situating at the different coordination environment[44,46]. According to frequency-dependent ac susceptibilities, two different χ'' signals can be observed as the temperature is decreased, which demonstrates the possible presence of two relaxation processes corresponding to the high-frequency signals (fast relaxation phase) and the low-frequency signals (slow relaxation phase) (Supplementary Fig. S7). As shown in the Supplementary Figs. S8 and S9, the Cole-Cole plots show double-separated relaxation phases at low temperature and similar semicircles at high temperature, respectively. By fitting the data with a generalized Debye model[47] above 4.0 K, the α values were obtainted in the range of 0.25–0.56, and the energy barrier can be further estimated using the Arrhenius law, $\tau = \tau_0 \exp(U_{eff}/kT)$, giving the parameters $U_{eff} = 29.0$ K and $\tau_0 = 3.6 \times 10^{-6}$ s ($R = 0.9965$) (Supplementary Fig. S10 and Table S2). While the data of Cole-Cole plots can not be successfully fitted below 4.0 K for double relaxation process with an extended Debye model[7] due to the fact that the low frequency peaks of χ'' signals were not clearly shown within the available frequency range of the ac measurements.

Scanning tunneling microscopy (STM) investigations. As complex **1** has the interesting non-centrosymmetric structure, it may have intrinsic molecular dipole and respond to the external electronic field on surface. To better explore the conformation and assembling of this novel complex, STM investigations were performed since such technique has been successfully used to probe the adlayers of several triple-decker sandwich compounds[14,15,48–51]. In our system, the sole triple-decker complex **1** cannot be stably adsorbed on HOPG surface, as characterized by STM. Nevertheless, with the help of a supramolecular template formed by 1,3,5-tris(10-carboxydecyloxy)benzene (TCDB), complex **1** can be immobilized into the formed nano cavity. On HOPG, through the hydrogen bonding interactions between molecules, TCDB can form rectangular networks with the inner cavity size of 2.8 nm × 1.7 nm (Supplementary Fig. S7). Besides, the shape and cavity size can be tunable based on the guest molecules because of the flexibility of long alkyl chains in TCDB molecule. In our previous work, this supramolecular network has been widely used as molecular templates to host alien ensembles and as spatial confiners to control the chemical reactions[52]. For our present system, as shown in Fig. 3, at a mixing molar ratio of 1 : 2 (TCDB: complex **1**), one TCDB cavity can accommodate one complex **1** molecule, leading to form a TCDB/complex **1** binary structure. When the molar ratio is increased to 1 : 4 (TCDB: complex **1**), each TCDB network cavity can hold two triple-decker molecules, forming the TCDB/2 complex **1** assembly (Fig. 4).

Interestingly, the complex **1** can perform the selective adsorption on HOPG, depending on the applied electrical field. At a positive bias scanning condition (Figs. 3a and 4a), close-packed triple layers with square-shaped bright spots can be found on HOPG. On the basis of the attribution of tunneling current, the bright spots should be attributed to the triple-decker. In the present case, since the size ($m \times n$ = (1.4 ± 0.1) nm × (1.4 ± 0.1) nm) of the top part is similar to that of the individual Pc molecule[53], we suggest that the Pc units point toward the solution while the H_2L toward the HOPG surface, that is to say, the conformation of the triple-decker complex **1** at positive bias is the top Pc and the bottom H_2L. If the STM measurement is performed at the negative bias, there appears another assembly situation. Under the negative bias, we could observe that the assembled structure of the binary TCDB/complex **1** (Fig. 3c) was disordered, and particularly existing some defects marked by the white arrows in the TCDB/2 complex **1** structure (Fig. 4c). Furthermore, the shape of the bright spots has changed into the rectangular strips, with the measured size of $m' \times n' = (1.6 \pm 0.1)$ nm × (1.3 ± 0.1) nm, which is the same as the assembled structures of TTF[54]. Hence, it may be highly possible that the H_2L locates at the top and the Pc at the bottom, when performed at negative bias.

As displayed in Figs. 3e and 4e, when the STM tip was applied at a positive bias, it is rational that the H_2L part is stably adsorbed toward HOPG surface, with the dipole direction along the external applied field. Besides, because of the perfect symmetry of Pc molecule, the top conformation in this case is regularly assembled. By contrary, at the negative bias, the triple-decker complex **1** is apt to be adsorbed with the Pc molecule toward the HOPG surface (Figs. 3f and 4f). Importantly, since the top H_2L is a non-symmetric structure, it may allow free rotation in the upper space. Hence, for the binary structures, the top bright spots observed at a negative bias are irregularly arranged. It should be noted that we did not observe any defect for the top conformation in the TCDB/complex **1** structure, which may result from the enough space for the free rotation of each H_2L of complex **1** in TCDB cavity. But for the TCDB/2 complex **1** structure, the rotation of the top H_2L of the two complex molecules

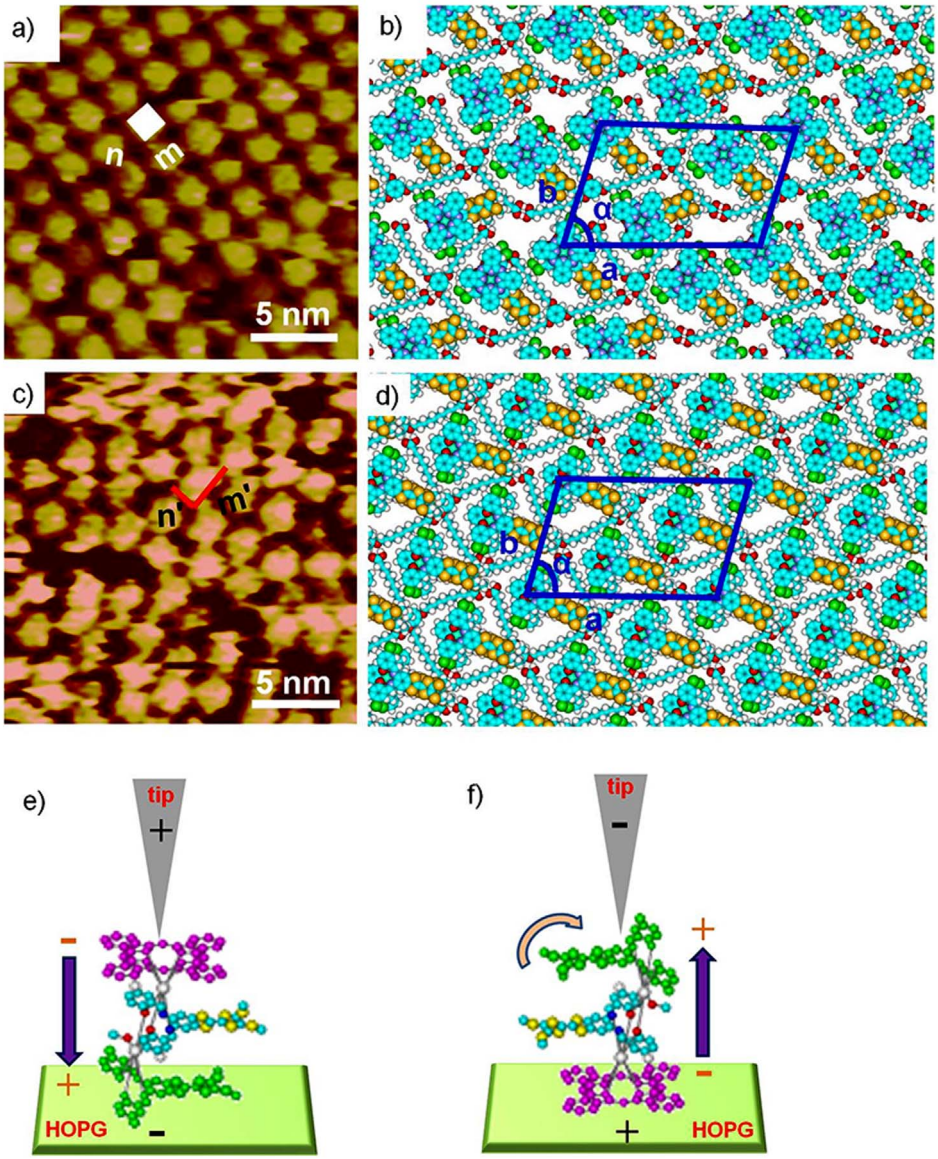

Figure 3 | (a, c) High resolution STM images of TCDB/complex **1** scanned at 700 mV and –500 mV, respectively. Tunneling parameter: I_{set} = 225.1 pA. (b, d) Suggested molecular models for the scanned structures in (a) and (c), respectively. (e, f) Tentative scheme models for illustrating the conformation of the complex **1** on HOPG surface at an applied positive bias and negative bias, respectively. To better illustrate the two different sides of the complex adsorbed on HOPG, we label the Pc part in purple and one H_2L unit in green (all H atoms are omitted). The linear arrows in the models represent the direction of dipolar and the electric property for the triple-decker complex **1**. The curved arrow displays the rotation of the top H_2L in 1-phenyloctane solution.

may be different, resulting in the contact and collision of top H_2L of the two complex molecules in a confined network during the rotation process, and thus losing some top H_2L parts.

Discussion

Based on these observed phenomena, the density functional theory (DFT) calculations have been performed to further investigate the target-molecule self-assembled structures on HOPG. The calculated lattice parameters for the TCDB/complex **1** self-assemblies are summarized in Table 1. It is clear that the calculated parameters of the theoretical models agree well with the experimental values. Meanwhile, we calculated the total energy and total energy per unit area for the TCDB/complex **1** system as shown in Table 2. The total energy includes the interaction between adsorbates (TCDB and complex **1**), and the interaction between adsorbates and graphite. Therefore, we could compare thermodynamic stability of the different networks by the total energy per unit area. Evidently, the total energies per unit area of the four kinds of assemblies are nearly equal. It means that the TCDB/complex **1** assembly and TCDB/2 complex **1** assembly, from the view point of thermodynamic, could be co-adsorbed under the same condition, which is consistent with the STM observation.

Furthermore, DFT calculations are performed to understand why the different patterns of complex **1** were recorded under the positive/negative STM bias though total energies per unit area of TCDB/complex **1** assemblies nearly equals that of TCDB/2 complex **1** assemblies. To explore the origin of such electrical field dependent selective adsorption, we investigate the interaction between the external electric field and intrinsic molecular properties. DFT results show that the triple-decker complex **1** is with intrinsic molecular dipole P (4.94 Debye), and the dipole moment directs from the Pc to the H_2L. When extra electrical field was applied, the extra stability energy E_{energy} could be calculated with the equation $E_{energy} = -P \cdot E_{external}$, which is caused by the interaction between the intrinsic molecular dipole P and the applied electric field $E_{external}$.

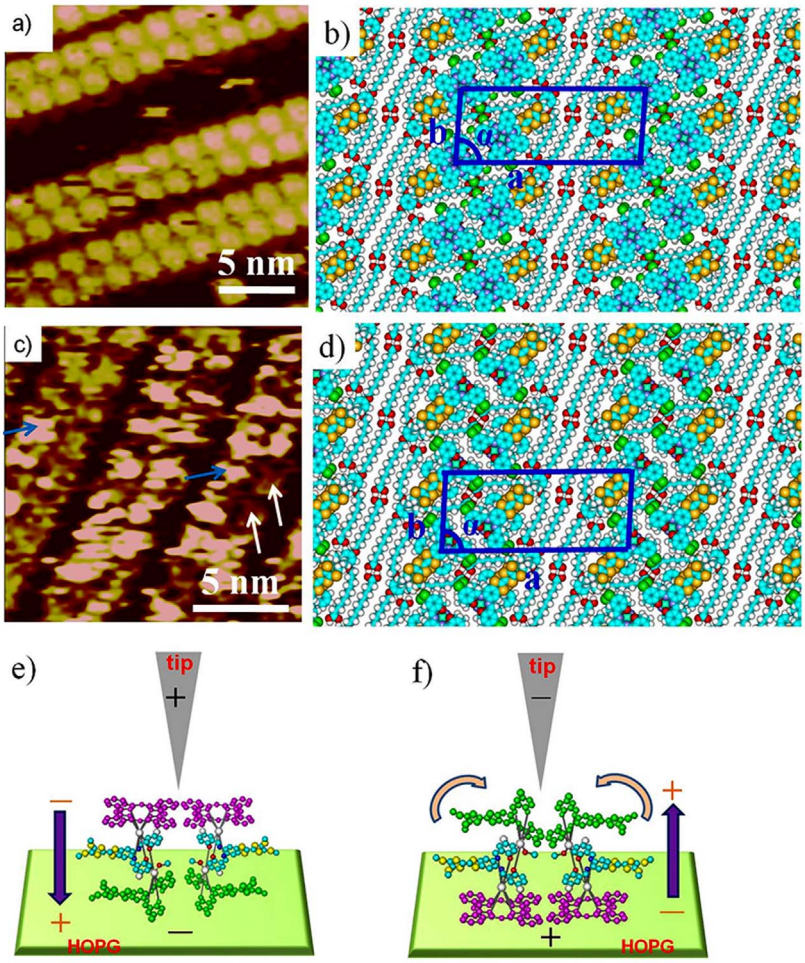

Figure 4 | (a, c) High resolution STM images for TCDB/2 complex **1** binary structure with the mixing molar ratio of 1:4. (a) Scanned at positive bias. I_{set} = 232.5 pA, V_{bias} = 743.1 mV. (c) Scanned at a negative bias. I_{set} = 232.5 pA, V_{bias} = −624.3 mV. (b) Suggested molecular models for the scanned structures in (a). (d) Suggested molecular models for the scanned structures in (c). (e, f) Tentative scheme models for illustrating the conformation of two complex **1** molecules on HOPG surface at an applied positive bias and negative bias, respectively. The linear arrows in the models represent the direction of dipolar and the electric property for the triple-decker complex **1**. The curved arrow displays the rotation of the top H_2L in 1-phenyloctane solution.

Considering that the distance between the STM tip and the substrate surface is 1 nm, the interaction between the molecular dipole and the external electric field could be calculated to be around 0.06 to 0.15 eV (with an applied bias ranging from ±0.60 V to ±1.50 V). In comparison with the thermal energy kT at room temperature (about 0.03 eV), this energy is significant and is considered sufficient to induce selective adsorption of the molecule in the electric field.

In summary, the unique triple-decker dinuclear lanthanide sandwich-type complex based on phthalocyanine and Schiff base ligand containing redox-active TTF unit is successfully synthesized, which has an interestingly non-centrosymmetric structure with two central Dy(III) ions situating in two different coordination geometries. The spectroscopic, electrochemical, and magnetic properties are fully investigated. More importantly, the assembling structures of this triple-decker compound on HOPG surface have been studied by STM, showing a bias dependent selective adsorption. By density function theory calculations, we reveal the formation mechanism of the molecular assemblies, and indicate that such electrical field

Table 1 | Experimental (Expt.) and calculated (Cal.) lattice parameters for the TCDB/complex 1 self-assemblies

			Unit cell parameters		
Assembled system	Adsorbed type		*a* (nm)	*b* (nm)	α (deg)
TCDB/complex **1**	Pc up	Expt.	4.9 ± 0.1	3.2 ± 0.1	74 ± 2
		Cal.	4.75	3.15	74
	H_2L up	Expt.	4.8 ± 0.2	2.8 ± 0.1	73 ± 2
		Cal.	4.50	2.90	74
TCDB/2 complex **1**	Pc up	Expt.	5.0 ± 0.1	1.9 ± 0.1	82 ± 2
		Cal.	4.92	2.00	85
	H_2L up	Expt.	4.7 ± 0.1	2.0 ± 0.1	83 ± 2
		Cal.	4.80	2.00	85

Table 2 | Total energies (E_{total}), and total energy per unit area for the observed TCDB/complex 1 self-assemblies. The total energy includes the interaction between adsorbates (TCDB and complex 1) and the interaction between adsorbates and graphite. Here, the more negative energy means the system is more stable

Assembled system	Adsorbed type	Total energies (kcal mol^{-1})	Total energy per unit area (kcal mol^{-1} nm^{-2})
TCDB/complex **1**	Pc up	−635.52	−44.19
	H_2L up	−642.13	−51.19
TCDB/2 complex **1**	Pc up	−494.73	−50.47
	H_2L up	−499.84	−52.27

dependent selective adsorption may be regulated by the interaction between the external electric field and intrinsic molecular properties including molecular dipole, electronics, and symmetry. The synthetic strategy, reported in this paper of introducing TTF unit into the sandwich-type Ln-Pc system, provides a possible route for preparing new multifunctional molecular materials. Moreover, it can be envisioned that such electrical-field-induced selective assembly will be of interest for preparing electrical molecular devices.

Methods

Details of the synthesis and characterization methods of compound **1** was described in the Supplementary Information. The crystallographic data and the bond lengths and bond angles are listed in Supplementary Tables S3 and S4 in the Supplementary Information. CCDC reference number 964624 (**1**).

TCDB and complex **1** were dissolved in 1-phenyloctane with concentration less than 10^{-4} M. A droplet (0.4 μL) of the 1-phenyloctane solution containing TCDB/complex **1** mixture (1 : 2 or 1 : 4) was deposited onto a freshly cleaved surface (5 mm × 5 mm) of HOPG, respectively. A few minutes later, the sample was studied by STM at a positive bias. After imaging the ordered structures, the bias was changed to a negative direction, and the STM images were captured again. It should be noted that it takes a few minutes to obtain stable assembled structures when changing the bias, this may result from the adsorption/desorption process of the complex **1** at surface.

The STM measurements were performed on a Nano IIIa scanning probe microscope system (Bruker, USA) under ambient conditions. All STM images were recorded in constant current mode using a mechanically cut Pt/Ir (80/20) tip.

Periodic theoretical calculations are performed using density functional theory (DFT) provided by the DMol^3 code[55]. The periodic boundary conditions (PBC) is used to describe the 2D periodic structure on the graphite in this work. The Perdew and Wang parameterization of the local exchange correlation energy are applied in local spin density approximation (LSDA) to describe exchange and correlation[56]. We expand the all-electron spin-unrestricted Kohn–Sham wave functions in a local atomic orbital basis. For the large system, the numerical basis set is applied. All calculations are all-electron ones, and performed with the medium mesh. Self-consistent field procedure is done with a convergence criterion of 10^{-5} a.u. on the energy and electron density.

1. Sessoli, R., Gatteschi, D., Caneschi, A. & Novak, M. A. Magnetic bistability in a metal-ion cluster. *Nature* **365**, 141–143 (1993).
2. Saitoh, E., Miyajima, H., Yamaoka, T. & Tatara, G. Current-induced resonance and mass determination of a single magnetic domain wall. *Nature* **432**, 203–206 (2004).
3. Bogani, L. & Wernsdorfer, W. Molecular spintronics using single-molecule magnets. *Nat. Mater.* **7**, 179–186 (2008).
4. Leuenberger, M. N. & Loss, D. Quantum computing in molecular magnets. *Nature* **410**, 789–793 (2001).
5. Troiani, F. & Affronte, M. Molecular spins for quantum information technologies. *Chem. Soc. Rev.* **40**, 3119–3129 (2011).
6. Ishikawa, N. *et al.* Lanthanide double-decker complexes functioning as magnets at the single-molecular level. *J. Am. Chem. Soc.* **125**, 8694–8695 (2003).
7. Katoh, K. *et al.* Multiple-decker phthalocyaninato dinuclear lanthanoid(III) single-molecule magnets with dual-magnetic relaxation processes. *Dalton Trans.* **41**, 13582–13600 (2012).
8. Wang, H. *et al.* A sandwich-type phthalocyaninato metal sextuple-decker complex: synthesis and NLO properties. *Chem. Commun.* **49**, 889–891 (2013).
9. Shang, H. *et al.* Sandwich-type tetrakis(phthalocyaninato) rare earth(III)-cadmium(II) quadruple-deckers. The effect of f-electrons. *Dalton Trans.* **42**, 1109–1115 (2013).
10. Kan, J. *et al.* Sandwich-type mixed tetrapyrrole rare-earth triple-decker compounds. Effect of the coordination geometry on the single-molecule-magnet nature. *Inorg. Chem.* **52**, 8505–8510 (2013).
11. Pushkarev, V. E. *et al.* Sandwich double-decker lanthanide(III) "intracavity" complexes based on clamshell-type phthalocyanine ligands: synthesis, spectral, electrochemical, and spectroelectrochemical investigations. *Chem. Eur. J.* **18**, 9046–9055 (2012).
12. Chen, Y. *et al.* High performance organic field-effect transistors based on amphiphilic tris(phthalocyaninato) rare earth triple-decker complexes. *J. Am. Chem. Soc.* **127**, 15700–15701 (2005).
13. Chen, Y. *et al.* Effect of peripheral hydrophobic alkoxy substitution on the organic field effect transistor performance of amphiphilic tris(phthalocyaninato) europium triple-Decker complexes. *Langmuir* **23**, 12549–12554 (2007).
14. Jiang, J. Z. & Ng, D. K. P. A decade journey in the chemistry of sandwich-type tetrapyrrolato rare earth complexes. *Acc. Chem. Res.* **42**, 79–88 (2009).
15. Katoh, K., Isshiki, H., Komeda, T. & Yamashita, M. Multiple-decker phthalocyaninato Tb(III) single-molecule magnets and Y(III) complexes for next generation devices. *Coord. Chem. Rev.* **255**, 2124–2148 (2011).
16. Katoh, K., Isshiki, H., Komeda, T. & Yamashita, M. Molecular spintronics based on single-molecule magnets composed of multiple-decker phthalocyaninato terbium(III) complex. *Chem. Asian. J.* **7**, 1154–1169 (2012).
17. Jurow, M. J. *et al.* Controlling morphology and molecular packing of alkane substitutedphthalocyanine blend bulk heterojunction solar cells. *J. Mater. Chem. A* **1**, 1557–1565 (2013).
18. Gonidec, M. *et al.* Surface supramolecular organization of a terbium(III) double-decker complex on graphite and its single molecule magnet behavior. *J. Am. Chem. Soc.* **133**, 6603–6612 (2011).
19. Ye, T. *et al.* Tuning interactions between ligands in self-assembled double-decker phthalocyanine arrays. *J. Am. Chem. Soc.* **128**, 10984–10985 (2006).
20. Cornia, A., Mannini, M., Sainctavit, P. & Sessoli, R. Chemical strategies and characterization tools for the organization of single molecule magnets on surfaces. *Chem. Soc. Rev.* **40**, 3076–3091 (2011).
21. Kubo, K. *et al.* Electronic state of a conducting single molecule magnet based on Mn-salen type and Ni-dithiolene Complexes. *Inorg. Chem.* **50**, 9337–9344 (2011).
22. Kosaka, Y. *et al.* Coexistence of conducting and magnetic electrons based on molecular π-electrons in the supramolecular conductor (Me-3,5-DIP)$[Ni(dmit)_2]_2$. *J. Am. Chem. Soc.* **129**, 3054–3055 (2007).
23. Hiraga, H. *et al.* Hybrid molecular material exhibiting single-molecule magnet behavior and molecular conductivity. *Inorg. Chem.* **46**, 9661–9671 (2007).
24. Coronado, E. & Day, P. Magnetic molecular conductors. *Chem. Rev.* **104**, 5419–5448 (2004).
25. Sugawara, T., Komatsu, H. & Suzuki, K. Interplay between magnetism and conductivity derived from spin-polarized donor radicals. *Chem. Soc. Rev.* **40**, 3105–3118 (2011).
26. Lorcy, D., Bellec, N., Fourmigué, M. & Avarvari, N. Tetrathiafulvalene-based group XV ligands: Synthesis, coordination chemistry and radical cation salts. *Coord. Chem. Rev.* **253**, 1398–1438 (2009).
27. Rosokha, S. V. & Kochi, J. K. Molecular and electronic structures of the long-bonded π-dimers of tetrathiafulvalene cation-radical in intermolecular electron transfer and in (solid-state) conductivity. *J. Am. Chem. Soc.* **129**, 828–838 (2007).
28. Coronado, E. *et al.* Molecular conductors based on the mixed-valence polyoxometalates $[SMo_{12}O_{40}]^{n-}$ (n = 3 and 4) and the organic donors bis(ethylenedithio)tetrathiafulvalene and bis(ethylenedithio)tetraselenafulvalene. *Inorg. Chem.* **48**, 11314–11324 (2009).
29. Shirahata, T. *et al.* Structural transitions from triangular to square molecular arrangements in the quasi-one-dimensional molecular conductors $(DMEDO\text{-}TTF)_2XF_6$ (X = P, As, and Sb). *J. Am. Chem. Soc.* **134**, 13330–13340 (2012).
30. Jeppesen, J. Q. *et al.* Amphiphilic bistable rotaxanes. *Chem. Eur. J.* **9**, 2982–3007 (2003).
31. Tseng, H.-R., Vignon, S. & Stoddart, J. F. Toward Chemically Controlled Nanoscale Molecular Machinery. *Angew. Chem., Int. Ed.* **42**, 1491–1495 (2003).
32. Enoki, T. & Miyazaki, A. Magnetic TTF-based charge-transfer complexes. *Chem. Rev.* **104**, 5449–5478 (2004).
33. Narayan, T. C., Miyakai, T., Seki, S. & Dinca, M. High charge mobility in a tetrathiafulvalene-based microporous metal-organic framework. *J. Am. Chem. Soc.* **134**, 12932–12935 (2012).
34. Pointillart, F., Golhen, S., Cador, O. & Ouahab, L. Paramagnetic 3d coordination complexes involving redox-active tetrathiafulvalene derivatives: an efficient approach to elaborate multi-properties materials. *Dalton Trans.* **42**, 1949–1960 (2013).
35. Pointillart, F. *et al.* Slow magnetic relaxation in radical cation tetrathiafulvalene-based lanthanide(III) dinuclear complexes. *Chem. Commun.* **49**, 11632–11634 (2013).
36. Pointillart, F. *et al.* Lanthanide dinuclear complexes involving tetrathiafulvalene-3-pyridine-N-oxide ligand: Semiconductor radical salt, magnetic, and photophysical studies. *Inorg. Chem.* **52**, 1398–1408 (2013).

37. Pointillart, F. *et al.* A series of tetrathiafulvalene-based lanthanide complexes displaying either single molecule magnet or luminescence—direct magnetic and photo-physical correlations in the ytterbium analogue. *Inorg. Chem.* **52**, 5978–5990 (2013).
38. Cosquer, G. *et al.* Slow magnetic relaxation in condensed versus dispersed dysprosium (III) mononuclear complexes. *Chem. Eur. J.* **139**, 7895–7903 (2013).
39. Pointillart, F. *et al.* High nuclearity complexes of lanthanide involving tetrathiafulvalene ligands: structural, magnetic, and photoPhysical properties. *Inorg. Chem.* **52**, 1610–1620 (2013).
40. Pointillart, F. *et al.* Single-molecule magnet behaviour in a tetrathiafulvalene-based electroactive antiferromagnetically coupled dinuclear dysprosium(III) complex. *Chem. Eur. J.* **17**, 10397–10404 (2011).
41. Alvarez, S. *et al.* Shape maps and polyhedral interconversion paths in transition metal chemistry. *Coord. Chem. Rev.* **249**, 1693–1708 (2005).
42. Wang, H. *et al.* Synthesis, structure, and single-molecule magnetic properties of rare-earth sandwich complexes with mixed phthalocyanine and schiff base ligands. *Chem. Eur. J.* **19**, 2266–2270 (2013).
43. Abbas, G. *et al.* Series of isostructural planar lanthanide complexes $[Ln^{III}_4(\mu_3\text{-}OH)_2(mdeaH)_2\text{-}(piv)_8]$ with single molecule magnet behavior for the Dy_4 analogue. *Inorg. Chem.* **49**, 8067–8072 (2010).
44. Gao, F. *et al.* A sandwich-type triple-decker lanthanide complex with mixed phthalocyanine and Schiff base ligands. *Dalton Trans.* 42, 11043–11046 (2013).
45. Osa, S. *et al.* A tetranuclear 3d−4f single molecule magnet: $[Cu^{II}LTb^{III}(hfac)_2]_2$. *J. Am. Chem. Soc.* **126**, 420–421 (2004).
46. Ke, H. *et al.* A linear tetranuclear dysprosium(III) compound showing single-molecule magnet behaviour. *Chem. Commun.* **46**, 6057–6059 (2010).
47. Katoh, K. *et al.* Magnetic relaxation of single-molecule magnets in an external magnetic field: an ising dimer of a terbium (III)–phthalocyaninate triple-decker complex. *Chem. Eur. J.* **17**, 117–122 (2011).
48. Lei, S. B. *et al.* Electric driven molecular switching of asymmetric tris(phthalocyaninato) lutetium triple-decker complex at the liquid/solid interface. *Nano Lett.* **8**, 1836–1843 (2008).
49. Yoshimoto, S., Sawaguchi, T., Su, W., Jiang, J. Z. & Kobayashi, N. Superstructure formation and rearrangement in the adlayer of a rare-earth-metal triple-decker sandwich complex at the electrochemical interface. *Angew. Chem., Int. Ed.* **46**, 1071–1074 (2007).
50. Ecija, D. *et al.* Assembly and manipulation of rotatable cerium porphyrinato sandwich complexes on a surface. *Angew. Chem., Int. Ed.* **50**, 3872–3877 (2011).
51. Vijayaraghavan, S. *et al.* Selective supramolecular fullerene-porphyrin interactions and switching in surface-confined C-60-Ce(tpp)(2) dyads. *Nano Lett.* **12**, 4077–4083 (2012).
52. Zhang, X. M., Zeng, Q.-D. & Wang, C. Molecular templates and nano-reactors: two-dimensional hydrogen bonded supramolecular networks on solid/liquid interfaces. *RSC Adv.* **3**, 11351–11366 (2013).
53. Liu, L. *et al.* Chaperon-mediated single molecular approach toward modulating Aβ peptide aggregation. *Nano Lett.* **9**, 4066–4072 (2009).
54. Abdel-Mottaleb, M. M. S. *et al.* Adlayers and low-dimensional assemblies of a TTF derivative at a liquid-solid interface. *Nano Lett.* **3**, 1375–1378 (2003).
55. Delley, B. From molecules to solids with the $DMol^3$ approach. *J. Chem. Phys.* **113**, 7756–7764 (2000).
56. Perdew, J. P. & Wang, Y. Accurate and simple analytic representation of the electron-gas correlation energy. *Phys. Rev. B* **45**, 13244–13249 (1992).

Acknowledgments

The authors thank the Major State Basic Research Development Program (2011CB808704, 2013CB922101, 2012CB933001 and 2011CB932303), and the National Natural Science Foundation of China (51173075, 51173031 and 91127043). The authors thank Dr. Jonathon E. Beves in the University of New South Wales (UNSW) for his valuable suggestions and help on this work.

Author contributions

J.-L.Z. and Q.-D.Z. contributed to the conception and design of the experiments, analysis of the data and revised the paper. F.G. and L.C. carried out the synthetic experiments and characterization. K.D. performed the theoretical computation and analysis. X.-M.Z. designed and carried out the STM experiments, analyzed the data. F.G. and X.-M.Z. wrote the paper.

Additional information

Supplementary information accompanies this paper at http://www.nature.com/scientificreports

Competing financial interests: The authors declare no competing financial interests.

How to cite this article: Gao, F. *et al.* Tetrathiafulvalene-Supported Triple-Decker Phthalocyaninato Dysprosium(III) Complex: Synthesis, Properties and Surface Assembly. *Sci. Rep.* **4**, 5928; DOI:10.1038/srep05928 (2014).